



NIH PUBLIC ACCESS

Author Manuscript

J Thromb Haemost. Author manuscript; available in PMC 2015 January 01.

Published in final edited form as:

J Thromb Haemost. 2014 January ; 12(1): 71–81. doi:10.1111/jth.12442.

Contributions of thrombin targets to tissue factor-dependent metastasis in hyperthrombotic mice

Naho Yokota^{*}, Alessandro Zarpellon[†], Sagarika Chakrabarty^{*}, Vladimir Y. Bogdanov[‡], András Gruber[§], Francis J. Castellino[¶], Nigel Mackman^{**}, Lesley G. Ellies^{††}, Hartmut Weiler^{‡‡}, Zaverio M. Ruggeri[†], and Wolfram Ruf^{*}

^{*}Department of Immunology and Microbial Science, The Scripps Research Institute, La Jolla, CA

[†]Department of Molecular and Experimental Medicine, The Scripps Research Institute, La Jolla, CA

[‡]Division of Hematology/Oncology, University of Cincinnati College of Medicine, Cincinnati, OH

[§]Departments of Biomedical Engineering and Medicine, Oregon Health and Science University, Portland, OR

[¶]W. M. Keck Center for Transgene Research, University of Notre Dame, IN

^{**}Department of Medicine, University of North Carolina, Chapel Hill, NC

^{††}Department of Pathology, University of California San Diego, La Jolla, CA

^{‡‡}Blood Research Institute, Blood Center of Wisconsin, Milwaukee, WI

Abstract

Background—Tumor cell tissue factor (TF)-initiated coagulation supports hematogenous metastasis by fibrin formation, platelet activation, and monocyte/macrophage recruitment. Recent studies identified host anticoagulant mechanisms as a major impediment for successful hematogenous tumor cell metastasis.

Objective—Here we address mechanisms that contribute to enhanced metastasis in hyperthrombotic mice with functional thrombomodulin deficiency (TM^{Pro} mice).

Methods—Pharmacological and genetic approaches were combined to characterize relevant thrombin targets in a mouse model of experimental hematogenous metastasis.

Results—TF-dependent, but contact pathway-independent syngeneic breast cancer metastasis was associated with marked platelet hyper-reactivity and formation of leukocyte-platelet aggregates in immune-competent TM^{Pro} mice. Blockade of CD11b or genetic deletion of platelet glycoprotein Iba excluded contributions of these receptors to enhanced platelet-dependent metastasis in hyperthrombotic mice. Mice with very low levels of the endothelial protein C receptor (EPCR) did not phenocopy the enhanced metastasis seen in TM^{Pro} mice. Genetic deletion of the thrombin receptor PAR1 or endothelial thrombin signaling targets alone did not diminish enhanced metastasis in TM^{Pro} mice. Combined deficiency of PAR1 on tumor cells and the host reduced metastasis in TM^{Pro} mice.

Correspondence: Wolfram Ruf, M.D., Department of Immunology and Microbial Science, SP258, The Scripps Research Institute, La Jolla, CA 92037, USA, Tel: 858-784-2748, FAX: 858-784-8480, ruf@scripps.edu.

Author contributions: N. Yokota performed research and wrote the paper; A. Zarpellon, S. Chakrabarty performed research; V. Y. Bogdanov, A. Gruber, F. J. Castellino, N. Mackman, L. G. Ellies, H. Weiler provided critical reagents and advice, Z. M. Ruggeri, W. Ruf designed experiments, interpreted data and edited the manuscript.

Conclusions—Metastasis in the hyperthrombotic TM^{Pro} mouse model is mediated by platelet hyper-reactivity and contributions of PAR1 signaling on tumor and host cells.

Keywords

Tissue Factor; Thrombin; Hypercoagulability; Metastasis; Platelets

Introduction

A prothrombotic state is one of the hallmarks of malignancies. Tissue factor (TF), the cellular initiator of the coagulation cascade, triggers local and remote thrombotic complications in cancer patients [1]. TF-dependent thrombin generation influences multiple cellular interactions in tumor microenvironments [2]. In spontaneous breast cancer progression and human xenograft models in the microenvironment of the mammary gland, tumor cell-expressed TF is important for gene expression patterns that regulate angiogenesis and tumor growth. These effects are thrombin-independent and involve cell signaling mediated by the TF cytoplasmic domain, activation of the protease activated receptor (PAR) 2, and integrin ligation [3–5]. TF also plays a role during intravasation of tumor cells, an important first step in tumor dissemination to distant sites [6]. In contrast to primary tumor growth, TF procoagulant activity is crucial for successful metastasis [7] by improving intravascular tumor cell survival through fibrin formation [8], platelet-dependent protection from natural killer cell attack [9;10], and priming of the metastatic niche to facilitate monocyte/macrophage interactions with tumor-associated microthrombi [11]. The platelet thrombin receptors glycoprotein (GP) Iba [12] and PAR4 [10] contribute to metastasis. In addition, the thrombin receptor PAR1 expressed by melanoma cells contributes to experimental metastasis [13;14], but deletion of PAR1 has no measurable effect on spontaneous metastasis in other tumor models [15].

Genetic or pharmacological perturbations of clinically relevant host anticoagulant mechanisms in mice influence the efficiency of metastasis. Vascular overexpression of the endothelial cell protein C receptor (EPCR) or treatment with activated protein C (aPC) reduces metastasis, whereas blocking endogenous aPC increases metastasis associated with endothelial barrier disruption [16;17]. Consistent with local anticoagulant control of tumor cell generated thrombin, mice carrying the aPC-resistant factor V_{Leiden} show increased hematogenous metastasis [18]. In addition, spontaneous and experimental metastasis is markedly enhanced in thrombomodulin Glu⁴⁰⁴/Pro mutant (TM^{Pro}) mice [19] that mimic inflammation-induced functional thrombomodulin deficiency by exhibiting reduced thrombin binding and PC activation [20]. Deficiency of thrombomodulin reduces generation of thrombin-activated fibrinolysis inhibitor (TAFI), but TAFI-deficient mice have no apparent alterations in metastasis [21]. Taken together with the crucial role of prothrombin for enhanced metastasis in TM^{Pro} mice [19], these studies suggest that thrombin neutralization by the endothelium and/or local aPC generation counteract tumor cell prometastatic abilities, but the downstream targets for thrombin remain incompletely defined.

Understanding prometastatic mechanisms in murine models has clinical implications for deciphering roles of the hemostatic system and prothrombotic states in tumor progression. Since factor VIII and von Willebrand Factor (vWF) are important for metastasis [18;22], we here evaluated the relative contributions of contact and TF pathway initiation to experimental hematogenous metastasis. We further analyzed the role of platelet receptors in the pro-metastatic phenotype of TM^{Pro} mice and capitalized on the unique absence of PAR1 from murine platelets [23] to identify PAR1 signaling on both tumor and host cells as a contributor to metastasis in hyperthrombotic TM^{Pro} mice.

Materials and Methods

Materials

Rat IgG2b anti-mouse CD11b antibody (M1/70), rat IgG1 anti-mouse PSGL-1 antibody (4RA10), and rat IgG2b control antibody (LTF-2) was purchased from BioXCell (West Lebanon, NH). The anti-thrombotic mouse anti-mouse factor (F) XI (14E11) monoclonal antibody blocks the activation of FXI by FXIIa [24] and is a potent inhibitor of thrombosis in contact pathway dependent models of thrombosis formation in mice [25]. Annexin 5 was expressed (plasmid a kind gift from Dr. Martin (The Smurfit Institute, Dublin, Ireland)), purified and labeled with Alexa488. Rat anti-mouse GPIIb α antibody (5A7) was raised against recombinant mouse GPIIb α ectodomain, screened for selectivity of mouse versus human GPIIb α , and confirmed for activity to deplete platelets in vivo. Alexa 647 rat IgG2a anti-mouse TF (21E10) and rabbit anti-mouse TF polyclonal antibody (R8084) were used for FACS and Western-blotting, respectively [25].

Tumor models

Mammary carcinoma cells (line 3503) were established from PyMT-TF^{flox} mice generated by crossing TF^{flox} and PyMT mice on a C57BL/6 background [26;27]. PyMT-TF^{flox} cells were transduced with adenovirus vector expressing cre recombinase on two consecutive days to delete TF. The TF knockout cells were reconstituted with murine full-length or alternatively-spliced TF (asTF) using pRetroX-IRES-DsRedExpress Vector (Clontech Laboratories, Mountain View, CA), as described [3]. Reconstitution was confirmed by Western blotting of whole cell lysates and supernatants fractionated into microparticles (MP) and soluble fractions. PAR1^{-/-} cells were established from independent PyMT PAR1^{-/-} mice, as described [15]. Cells were cultured in L-15 medium with 10% FCS, 10 μ g/ml insulin, and 10 mM L-glutamine.

Mice

Animal experiments were performed under approved protocols of the Institutional Animal Care and Use Committee (IACUC) of the Scripps Research Institute. Mice were backcrossed into the C57BL/6 strain. EPCR^{low} hypomorphic mice express very low levels of EPCR [28]. TM^{Pro} mice [20] were crossed with PAR1^{-/-} mice [15;29] or *Slc7a2*^{-/-} mice [30] to generate TM^{Pro}/*Slc7a2*^{-/-} mice and TM^{Pro}/PAR1^{-/-} mice, respectively. Platelets were isolated from murine GPIIb α -deficient mice that carried transgenes for platelet-specific expression of either human GPIIb α or a chimeric molecule in which the extracellular domain of GPIIb α was replaced by the IL-4 receptor ectodomain (IL-4R).

Experimental hematogenous metastasis model

Typically, 8×10^4 PyMT-TF^{flox} cells were injected into the lateral tail vein of TM^{Pro} mice and 2×10^5 cells into other strains that did not carry the TM mutation and mice were sacrificed after 21 days. For PyMT-PAR1^{-/-} cells (2×10^5 cells/mouse), metastasis was scored after 35 days. The wet lung weights were recorded and lungs were fixed in Bouin's solution for counting tumor foci on the lung surface.

Tumor cell quantification in lungs

Tumor cell retention in the lungs was measured 24 hours after injection. Minced lung tissue (20 mg) was extracted in 500 μ l of alkaline lysis buffer (25 mM NaOH, 0.2 mM EDTA, pH 12) overnight at 95°C, neutralized with 500 μ l 40 mM Tris-HCl, pH 5, and 10 μ l of lung DNA sample or DNA extracted from a defined numbers of tumor cells were used for Taqman amplification of the PyMT transgene using forward primer 5'-CTGAGCCCCGATGACAGCATA-3', reverse primer 5'-

TCTTGGTCGCTTTCTGGATACA, and the Taqman probe 5'-[6-FAM]CCCCGGACCCCCCAGAAGT[tamra-Q]-3'. Tumor cells in the lungs were quantified based on the tumor cell standard and total lung weights.

Antibody treatments and fibrinogen depletion

Mice were given intraperitoneal injections of 2 $\mu\text{g/g}$ body weight of anti-FXI antibody 14E11, 100 μg of monoclonal anti-GPIIb α antibody 5A7, 200 μg of monoclonal anti-CD11b antibody M1/70, 100 μg of monoclonal anti-PSGL-1 (CD162) antibody, or the same doses of control IgG at 4 and 24 hours prior to the tumor cell inoculation. Fibrinogen was depleted by intravenous injection of 25 KU/kg recombinant batroxobin (Creative Biomart, NY) from the snake venom of *Bothrops atrox* [31], 1 hour prior to tumor cell injection. Fibrinogen depletion was monitored spectrophotometrically by absorbance changes at 350 nm of 100 μl of 10-fold diluted citrated plasma samples mixed with 100 μl of thrombin (100 nM).

Platelet experiments

Platelets were depleted with anti-mouse GPIIb α antibody (5A7) prior to reconstitution with platelets expressing human GPIIb α (hGPIIb α) or IL-4R, both of which were not affected by the depleting antibody. For platelet preparation, blood was collected from the retro-orbital plexus of anesthetized mice and mixed with one-tenth volume 3.2% sodium citrate and diluted in Tyrode's solution pH 6.5 for isolation of platelets that were resuspended in Tyrode's solution, pH 7.4 for intravenous injection at doses of 4–6 $\times 10^8$ /mouse. Mouse platelets were stained with annexin 5 in diluted whole blood (1:100 in Tyrode's Buffer, 5 mM CaCl₂ versus 10 mM EDTA negative controls) obtained from untreated mice or 2 hours after injection of 2 $\times 10^5$ PyMT-TF^{flox} cells or buffer and analyzed with a LSRII, using gating based on size and collection of a minimum of 10,000 events. Platelet-leukocyte aggregates (PLA) were quantified in diluted whole blood stained with anti-mouse CD45 and CD42b as double positive events in the CD45 population. Platelet counts were obtained with a Hemavet 950LV hematological analyzer (Drew Scientific, Dallas, TX).

Functional characterization of tumor cells

FXa generation was measured on cell monolayers using a discontinuous chromogenic assay with Spectrozyme FXa (American Diagnostica, Stamford, CT). Western blotting used a rabbit anti-mouse TF polyclonal antibody (8084) and integrin $\beta 1$ or β actin as loading controls.

Statistical analysis

Data are presented as mean \pm SD. We used GraphPad Prism version 4.03 for the Student unpaired *t* test and analysis of variance (ANOVA). Multiple comparisons by ANOVA included the Bonferroni posttest.

Results

TF-dependent metastasis in TM^{Pro} mice is independent of the contact pathway

We have used the PyMT model of spontaneous murine breast cancer development to study TF-dependent primary tumor growth [3;15]. Similar to various other tumor models [19], PyMT breast cancer cells injected at the same dose metastasized more efficiently in TM^{Pro} mice (Fig. 1A). To confirm the procoagulant contributions of tumor cell TF, we deleted TF from established metastatic PyMT-TF^{flox} breast cancer populations using *in vitro* treatment with cre recombinase. Western blotting (Fig. 1B), FACS analysis (Fig. 1C), and FXa generation assay (Fig. 1D) confirmed highly efficient deletion of TF. Pulmonary metastasis was markedly reduced following TF deletion and injection of the same number of TF-

depleted cells into WT or TM^{Pro} mice (Fig. 1E). Metastatic burden was insignificantly increased in TM^{Pro} mice relative to WT, which may be caused by the presence of alternative tumor procoagulants and/or conditioning of the metastatic niche due to the procoagulant state of TM^{Pro} mice [11]. TF-deficient cells were reconstituted with either full-length (fTF) or alternatively spliced TF (asTF) (Fig. 1F). Testing of these lines confirmed that procoagulant fTF, but not asTF [32] was required for metastasis (Fig. 1G). These data indirectly support the concept that asTF mainly promotes tumor progression through coagulation-independent effects on integrins in the context of tumor angiogenesis and primary tumor expansion [4;33;34].

The contact pathway contributes to TF-dependent thrombosis [24;25], but the role of the contact pathway in metastasis of hyperthrombotic TM^{Pro} mice is unknown. WT or TM^{Pro} mice were intravenously injected with PyMT-TF^{fllox} breast cancer cells at different doses, in order to compensate in part for the diminished metastasis in WT mice. We blocked FXIIa-mediated FXI activation with the anti-FXI antibody 14E11, given prior to tumor cell injection at an 8-fold higher dose than the one required for complete inhibition of experimental thrombosis [25]. This antibody had no effect on the markedly enhanced metastasis in TM^{Pro} mice (Fig. 1H). These results provided new evidence that tumor cell TF drives experimental metastasis independent of contact phase activation in TM^{Pro} mice.

Increased platelet activation in TM^{Pro} mice

TF-initiated thrombin generation supports tumor cell homing and survival through fibrin formation [8], but blockade of endogenous PC renders the metastatic process apparently independent of fibrinogen by poorly understood mechanisms [35]. Similarly, fibrinogen depletion by > 98% with a single dose (25KU/kg) of recombinant batroxobin attenuated metastasis in WT, but produced no statistically significant reduction in hyperthrombotic TM^{Pro} mice (Fig. 2A). These data indicated that the hypermetastatic phenotype of TM^{Pro} mice was not primarily caused by increased local fibrin network formation. Surprisingly, control experiments showed that fibrinogen depletion produced a marked drop in platelet counts specifically in TM^{Pro} mice (Fig. 2B). Platelet counts were indistinguishable between WT and TM^{Pro} mice at baseline and fibrinogen depletion had no effect on platelet counts in WT mice (Fig. 2B). These data indicate that fibrinogen deficiency produces complex effects in hyperthrombotic mouse models that make it difficult to study specific contributions of fibrinogen or fibrin to the metastatic process.

We reasoned that depletion of the abundant thrombin substrate and regulator fibrinogen [36] led to increased activation of platelets that in turn compensated for the decreased fibrinogen levels during metastasis. This conclusion raised the question whether platelet hyper-reactivity occurred following injection of procoagulant tumor cells. Platelet surface phosphatidylserine detected by annexin 5 staining was increased in TM^{Pro} mice under unchallenged conditions, but this platelet population was no longer seen after tumor cell injection (Fig. 2C). Instead, a drop in platelet counts (Fig. 2D) and markedly increased numbers of platelet-leukocyte aggregates (Fig. 2E) were observed following tumor cell injection specifically into TM^{Pro} mice. Thus, increased platelet activation is a previously unidentified effect of amplified thrombin generation in this hyperthrombotic mouse strain.

Leukocyte interaction with platelet GPIIb α is not required for enhanced metastasis in TM^{Pro} mice

Given the increased platelet-leukocyte aggregates and prior studies implicating both GPIIb α [12] and CD11b⁺ monocyte/macrophages interacting with blood clots in the efficiency of metastasis [11], we asked whether the interaction between platelet-expressed GPIIb α and CD11b [37] contributed to enhanced metastasis of breast cancer cells in TM^{Pro} mice. We

blocked CD11b with antibody M1/70 administered at a dose 4-fold higher than that previously used to inhibit myeloid cell recruitment in tumor growth experiments [38], and confirmed prior data that this antibody had no effect on leukocyte counts, but abolished CD11b staining on blood white blood cells isolated from specific antibody-treated mice. CD11b blockade had no effect on metastasis in the depicted and an independent experiment in TM^{Pro} mice (Fig. 3A).

In order to exclude redundancy in leukocyte recruitment pathways due to the hyper-reactive platelets of TM^{Pro} mice, we also blocked PSGL-1 (CD162), an important leukocyte counter-ligand for platelet P selectin. Note that PSGL-1 was not expressed by our tumor cells and that carbohydrate ligands on carcinoma cell mucins are known to initiate prometastatic, platelet-dependent pathways involving PSGL-1 [39]. Treating mice with anti-mouse PSGL-1 antibody at previously used inhibitory doses [40] alone or in combination with anti-CD11b antibody M1/70 (Fig. 3B) had no effect on metastasis in TM^{Pro} mice relative to control antibody-treated mice.

We used a genetic strategy to further address roles of platelet-expressed GPIb α as a counter-receptor for CD11b. We generated a monoclonal antibody (5A7) to murine GPIb α without cross-reactivity to human GPIb α and confirmed the efficiency of the antibody to achieve prolonged platelet depletion in WT mice for 24–48 hours (Fig. 3C). Depleted mice were transfused with platelets expressing either human GPIb α (hGPIb α) or a chimeric protein of the IL-4R extracellular domain replacing the murine GPIb α ectodomain to prevent the Bernard-Soulier phenotype of GPIb α -deficient platelets [41]. Reconstitution with either platelet source restored platelet counts in accordance with the administered dose (Fig. 3C). Depletion of platelets markedly reduced the number of tumor cells retained in the lungs 24 hours after injection and lung metastasis in WT mice (Fig. 3D, E) and metastasis in TM^{Pro} mice (Fig. 3E), as previously reported [19]. Reconstitution of platelet-depleted mice with platelets expressing either hGPIb α or the IL-4R chimera restored metastasis to similar levels (Fig. 3E), with an insignificant trend towards higher metastasis when depleted WT mice were reconstituted with GPIb α replete platelets expressing the human receptor. Thus, both pharmacological and genetic approaches found no contribution of the GPIb α -CD11b interaction to platelet-dependent metastasis in TM^{Pro} mice.

PAR1 signaling contributes to enhanced metastasis in TM^{Pro} mice

The mutation introduced in TM^{Pro} mice impairs both thrombin binding and activation of the PC pathway that is dependent on EPCR [20]. Endothelial overexpression of EPCR suppresses metastasis [16] and deficiency of EPCR increases vascular leak in inflammation [42], but metastasis was not enhanced in EPCR^{low} mice, in contrast to TM^{Pro} mice (Fig. 4A). Endothelial cell EPCR-aPC-PAR1 and thrombin-PAR1 signaling produce opposing gene expression changes, including the cationic amino acid transporter *Slc7a2*. *Slc7a2* is induced by thrombin, but downregulated by aPC signaling [43], and *Slc7a2* regulates nitric oxide production, previously implicated in tumor progression [27]. We tested whether loss of this thrombin-PAR1 signaling target attenuated metastasis. Metastasis in *Slc7a2*^{-/-} hosts was indistinguishable from WT controls and, importantly, *Slc7a2*-deletion did not correct the prometastatic phenotype of TM^{Pro} mice, as seen with platelet depletion (Fig. 4B). Thus, increased metastasis in TM^{Pro} mice was independent of EPCR and one of the possible downstream targets of endothelial cell thrombin-PAR1 signaling.

In the mouse, thrombin activates platelets through PAR4 and PAR1 expressed by other host cells is dispensable for metastasis in mice without coagulation abnormalities [10]. As seen with other tumor models [10], breast cancer cell metastasis was not significantly impaired in PAR1^{-/-} mice (Fig. 4C). In addition, metastasis was not different between TM^{Pro} and

TM^{Pro}/PAR1^{-/-} mice (Fig. 4D). Thus, loss of host thrombin-PAR1 signaling alone was insufficient to attenuate increased metastasis in TM^{Pro} mice.

In addition, tumor cell PAR1 signaling has been implicated in the prometastatic phenotype of melanoma cells [13;14]. We next addressed whether increased thrombin levels in TM^{Pro} mice increased metastasis through signaling involving PAR1 on tumor cells, using thrombin-insensitive breast cancer cell lines from PyMT-PAR1^{-/-} mice [15]. Two independent PyMT-PAR1^{-/-} cell populations expressed similar TF antigen (Fig. 5A, C) and activity (Fig. 5B). As seen with PAR1-expressing WT control, each of the PyMT-PAR1^{-/-} lines showed markedly enhanced metastasis in TM^{Pro} mice when the same cell dose was injected into mutant or WT mice (Fig. 5D). Thus, thrombin-mediated activation of PAR1 on tumor cells also did not account for enhanced metastasis in TM^{Pro} mice.

Endothelial cell PAR1 signaling induces the chemokine CCL2 (MCP-1) [44] that is pivotal for efficient metastasis [45]. Because both host- and tumor cell-derived CCL2 contribute to metastasis [45], we next addressed the possibility that host- and tumor cell-expressed PAR1 similarly played redundant roles in thrombin-dependent metastasis in TM^{Pro} mice. We first injected a fairly high tumor cell dose of PAR1-deficient tumor cells and found an insignificant trend towards decreased metastasis in PAR1^{-/-} mice (Fig. 5E). Moreover, metastasis of PAR1-deficient tumor cells injected into TM^{Pro}/PAR1^{-/-} was significantly reduced in two independent experiments relative to TM^{Pro} controls (Fig. 5E). However, the inhibitory effect of combined host and tumor cell PAR1 deficiency on the hypermetastatic phenotype of TM^{Pro} mice was only partial, suggesting that multiple thrombin targets contribute to enhanced metastasis in this hyperthrombotic mouse model.

Discussion

This study provides new insight into the roles of thrombin targets in enhancing TF-dependent metastasis in hyperthrombotic mice. We uncovered increased baseline PS exposure on platelets in TM^{Pro} mice and a marked increase in platelet-leukocyte aggregates following the prothrombotic challenge of injecting tumor cells. These results suggest that increased platelet activation can become a predominant prometastatic mechanism in prothrombotic states. Increased platelet-leukocyte aggregates were seen in mice with circulating tumor cells. We therefore assessed with pharmacological and genetic approaches the contributions of a key receptor interaction bridging platelets and leukocytes that had previously been implicated in metastasis, i.e. GPIIb/IIIa and CD11b [11;12][37].

We found no apparent contribution of these receptors to enhanced metastasis in TM^{Pro} mice. A subtle increase in metastasis was seen when WT mice were reconstituted with platelets expressing human GPIIb/IIIa versus IL-4R chimera platelets with normal size and shape, while complete GPIIb/IIIa deficiency had previously been shown to result in a pronounced decrease in metastasis [12]. Since genetic deficiency of CD11b also had a more pronounced effect on metastasis [11] that contrasted with the lack of inhibition by our short term pharmacological blockade of CD11b, it is tempting to speculate that leukocyte-platelet interactions in immune competent mouse models may influence metastasis by more long term effects on leukocyte populations and/or priming of metastatic niches. It will be of interest for future studies to study alternative pathways that support platelet-leukocyte interactions as well as address paracrine and adhesive interactions between tumor cells and platelets as potential factors that enhance metastasis in hyperthrombotic mouse models [46].

TM^{Pro} mice are defective in both aPC generation and local neutralization of thrombin generated intravascularly, but metastasis was neither enhanced by deletion of the aPC co-signaling receptor EPCR nor reduced in TM^{Pro} mice by genetic deletion of PAR1 on host

cells or PAR1 downstream endothelial targets. However, deficiency of PAR1 in both, tumor and host cells, reduced metastasis significantly. These data are in line with prior data that implicated tumor cell PAR1 in melanoma metastasis [13;14] and indicate that host and tumor cell PAR1 can mediate partially redundant functions in breast cancer cell metastasis. The PAR1-inducible and prometastatic chemokine CCL2 has redundant sites of synthesis in the tumor and host cell compartments [45], but more extensive studies will be required to determine whether CCL2 is one of the relevant PAR1 target during the metastatic process. Since PAR4, but not PAR1, is the relevant thrombin receptor on mouse platelets, the partial reduction of metastasis following PAR1 deletion in TM^{Pro} mice indicates that the hyperthrombotic state of TM^{Pro} mice favors multiple tumor-promoting pathways in addition to thrombin-driven interactions of platelets with tumor cells.

Acknowledgments

We thank Maki Kitano, Jennifer Royce and Pablito Tejada for excellent technical assistance. This study was supported by NIH grants HL-60742 (WR) and HL-42846 (ZMR).

References

1. Ruf W, Disse J, Carneiro-Lobo TC, Yokota N, Schaffner F. Tissue factor and cell signalling in cancer progression and thrombosis. *J Thromb Haemost.* 2011; 9(Suppl 1):306–15. [PubMed: 21781267]
2. Ruf W, Mueller BM. Thrombin generation and the pathogenesis of cancer. *Semin Thromb Hemost.* 2006; 32:61–8. [PubMed: 16673267]
3. Schaffner F, Versteeg HH, Schillert A, Yokota N, Petersen LC, Mueller BM, Ruf W. Cooperation of tissue factor cytoplasmic domain and PAR2 signaling in breast cancer development. *Blood.* 2010; 116:6106–13. [PubMed: 20861457]
4. van den Berg YW, van den Hengel LG, Myers HR, Ayachi O, Jordanova E, Ruf W, Spek CA, Reitsma PH, Bogdanov VY, Versteeg HH. Alternatively spliced tissue factor induces angiogenesis through integrin ligation. *Proc Natl Acad Sci U S A.* 2009; 106:19497–502. [PubMed: 19875693]
5. Versteeg HH, Schaffner F, Kerver M, Petersen HH, Ahamed J, Felding-Habermann B, Takada Y, Mueller BM, Ruf W. Inhibition of tissue factor signaling suppresses tumor growth. *Blood.* 2008; 111:190–9. [PubMed: 17901245]
6. Conn EM, Madsen MA, Cravatt BF, Ruf W, Deryugina EI, Quigley JP. Cell surface proteomics identifies molecules functionally linked to tumor cell intravasation. *J Biol Chem.* 2008; 283:26518–27. [PubMed: 18658134]
7. Mueller BM, Ruf W. Requirement for binding of catalytically active factor VIIa in tissue factor dependent experimental metastasis. *J Clin Invest.* 1998; 101:1372–8. [PubMed: 9525979]
8. Palumbo JS, Kombrinck KW, Drew AF, Grimes TS, Kiser JH, Degen JL, Bugge TH. Fibrinogen is an important determinant of the metastatic potential of circulating tumor cells. *Blood.* 2000; 96:3302–9. [PubMed: 11071621]
9. Nieswandt B, Hafner M, Echtenacher B, Mannel DN. Lysis of tumor cells by natural killer cells in mice is impeded by platelets. *Cancer Res.* 1999; 59:1295–300. [PubMed: 10096562]
10. Camerer E, Qazi AA, Duong DN, Cornelissen I, Advincola R, Coughlin SR. Platelets, protease-activated receptors, and fibrinogen in hematogenous metastasis. *Blood.* 2004; 104:397–401. [PubMed: 15031212]
11. Gil-Bernabe AM, Ferjancic S, Tlalka M, Zhao L, Allen PD, Im JH, Watson K, Hill SA, Amirhosravi A, Francis JL, Pollard JW, Ruf W, Muschel RJ. Recruitment of monocytes/macrophages by tissue factor-mediated coagulation is essential for metastatic cell survival and premetastatic niche establishment in mice. *Blood.* 2012; 119:3164–75. [PubMed: 22327225]
12. Jain S, Zuka M, Liu J, Russell S, Dent J, Guerrero JA, Forsyth J, Maruszak B, Gartner TK, Felding-Habermann B, Ware J. Platelet glycoprotein Ib alpha supports experimental lung metastasis. *Proc Natl Acad Sci U S A.* 2007; 104:9024–8. [PubMed: 17494758]

13. Villares GJ, Zigler M, Dobroff AS, Wang H, Song R, Melnikova VO, Huang L, Braeuer RR, Bar-Eli M. Protease activated receptor-1 inhibits the Maspin tumor-suppressor gene to determine the melanoma metastatic phenotype. *Proc Natl Acad Sci U S A*. 2011; 108:626–31. [PubMed: 21187389]
14. Shi X, Gangadharan B, Brass LF, Ruf W, Mueller BM. Protease-activated receptor 1 (PAR1) and PAR2 contribute to tumor cell motility and metastasis. *Mol Cancer Res*. 2004; 2:395–402. [PubMed: 15280447]
15. Versteeg HH, Schaffner F, Kerver M, Ellies LG, Andrade-Gordon P, Mueller BM, Ruf W. Protease activated receptor (PAR)2, but not PAR1 signaling promotes the development of mammary adenocarcinoma in PyMT mice. *Cancer Res*. 2008; 68:7219–27. [PubMed: 18757438]
16. Bezuhly M, Cullen R, Esmon CT, Morris SF, West KA, Johnston B, Liwski RS. Role of activated protein C and its receptor in inhibition of tumor metastasis. *Blood*. 2009; 113:3371–4. [PubMed: 19188668]
17. Van Sluis GL, Niers TM, Esmon CT, Tigchelaar W, Richel DJ, Buller HR, Van Noorden CJ, Spek CA. Endogenous activated protein C limits cancer cell extravasation through sphingosine-1-phosphate receptor 1-mediated vascular endothelial barrier enhancement. *Blood*. 2009; 114:1968–73. [PubMed: 19571314]
18. Bruggemann LW, Versteeg HH, Niers TM, Reitsma PH, Spek CA. Experimental melanoma metastasis in lungs of mice with congenital coagulation disorders. *J Cell Mol Med*. 2008; 12:2622–7. [PubMed: 18363839]
19. Horowitz NA, Blevins EA, Miller WM, Perry AR, Talmage KE, Mullins ES, Flick MJ, Queiroz KC, Shi K, Spek CA, Conway EM, Monia BP, Weiler H, Degen JL, Palumbo JS. Thrombomodulin is a determinant of metastasis through a mechanism linked to the thrombin binding domain but not the lectin-like domain. *Blood*. 2011; 118:2889–95. [PubMed: 21788337]
20. Weiler H, Lindner V, Kerlin B, Isermann B, Hendrickson S, Cooley B, Meh D, Mosesson M, Schworak N, Post M, Conway E, Ulfman L, Von Andrian UH, Weitz JI. Characterization of a mouse model for thrombomodulin deficiency. *Arterioscler Thromb Vasc Biol*. 2001; 21:1531–7. [PubMed: 11557684]
21. Reijerkerk A, Meijers JC, Havik SR, Bouma BN, Voest EE, Gebbink MF. Tumor growth and metastasis are not affected in thrombin-activatable fibrinolysis inhibitor-deficient mice. *J Thromb Haemost*. 2004; 2:769–79. [PubMed: 15099284]
22. Terraube V, Pendu R, Baruch D, Gebbink MF, Meyer D, Lenting PJ, Denis CV. Increased metastatic potential of tumor cells in von Willebrand factor-deficient mice. *J Thromb Haemost*. 2006; 4:519–26. [PubMed: 16405520]
23. Connolly AJ, Ishihara H, Kahn ML, Farese RV Jr, Coughlin SR. Role of the thrombin receptor in development and evidence for a second receptor. *Nature*. 1996; 381:516–9. [PubMed: 8632823]
24. Cheng Q, Tucker EI, Pine MS, Sisler I, Matafonov A, Sun MF, White-Adams TC, Smith SA, Hanson SR, McCarty OJ, Renne T, Gruber A, Gailani D. A role for factor XIIa-mediated factor XI activation in thrombus formation in vivo. *Blood*. 2010; 116:3981–9. [PubMed: 20634381]
25. Furlan-Freguia C, Marchese P, Gruber A, Ruggeri ZM, Ruf W. P2X7 receptor signaling contributes to tissue factor-dependent thrombosis in mice. *J Clin Invest*. 2011; 121:2932–44. [PubMed: 21670495]
26. Wang L, Miller C, Swarthout RF, Rao M, Mackman N, Taubman MB. Vascular smooth muscle-derived tissue factor is critical for arterial thrombosis after ferric chloride-induced injury. *Blood*. 2009; 113:705–13. [PubMed: 18931346]
27. Davie SA, Maglione JE, Manner CK, Young D, Cardiff RD, MacLeod CL, Ellies LG. Effects of FVB/NJ and C57Bl/6J strain backgrounds on mammary tumor phenotype in inducible nitric oxide synthase deficient mice. *Transgenic Res*. 2007; 16:193–201. [PubMed: 17206489]
28. Castellino FJ, Liang Z, Volkir SP, Haalboom E, Martin JA, Sandoval-Cooper MJ, Rosen ED. Mice with a severe deficiency of the endothelial protein C receptor gene develop, survive, and reproduce normally, and do not present with enhanced arterial thrombosis after challenge. *Thromb Haemost*. 2002; 88:462–72. [PubMed: 12353077]

29. Darrow AL, Fung-Leung W-P, Ye RD, Santulli RJ, Cheung W-M, Derian CK, Burns CL, Damiano BP, Zhou L, Keenan CM, Peterson PA, Andrade-Gordon P. Biological consequences of thrombin receptor deficiency in mice. *Thromb Haemost.* 1996; 76:860–6. [PubMed: 8972001]
30. Rothenberg ME, Doepker MP, Lewkowich IP, Chiaramonte MG, Stringer KF, Finkelman FD, MacLeod CL, Ellies LG, Zimmermann N. Cationic amino acid transporter 2 regulates inflammatory homeostasis in the lung. *Proc Natl Acad Sci U S A.* 2006; 103:14895–900. [PubMed: 17003120]
31. Matsui T, Fujimura Y, Titani K. Snake venom proteases affecting hemostasis and thrombosis. *Biochim Biophys Acta.* 2000; 1477:146–56. [PubMed: 10708855]
32. Bogdanov VY, Kirk RI, Miller C, Hathcock JJ, Vele S, Gazdoui M, Nemerson Y, Taubman MB. Identification and characterization of murine alternatively spliced tissue factor. *J Thromb Haemost.* 2006; 4:158–67. [PubMed: 16409465]
33. Srinivasan R, Ozhegov E, van den Berg YW, Aronow BJ, Franco RS, Palascak MB, Fallon JT, Ruf W, Versteeg HH, Bogdanov VY. Splice Variants of Tissue Factor Promote Monocyte-Endothelial Interactions by Triggering the Expression of Cell Adhesion Molecules via Integrin-Mediated Signaling. *J Thromb Haemost.* 2011; 9:2087–96. [PubMed: 21812913]
34. Kocaturk B, van den Berg YW, Tieken C, Mieog JSD, de Kruijf EM, Engels CC, van der Ent MA, Kuppen PJK, van de Velde CJ, Ruf W, Reitsma PH, Osanto S, Liefers GJ, Bogdanov VY, Versteeg HH. Alternatively spliced Tissue Factor promotes breast cancer growth in a B1 integrin-dependent manner. *Proc Natl Acad Sci U S A.* 2013; 110:11517–22. [PubMed: 23801760]
35. Van Sluis GL, Bruggemann LW, Esmon CT, Kamphuisen PW, Richel DJ, Buller HR, Van Noorden CJ, Spek CA. Endogenous activated protein C is essential for immunemediated cancer cell elimination from the circulation. *Cancer Lett.* 2011; 306:106–10. [PubMed: 21420234]
36. Kerlin B, Cooley BC, Isermann BH, Hernandez I, Sood R, Zogg M, Hendrickson SB, Mosesson MW, Lord S, Weiler H. Cause-effect relation between hyperfibrinogenemia and vascular disease. *Blood.* 2004; 103:1728–34. [PubMed: 14615369]
37. Wang Y, Sakuma M, Chen Z, Ustinov V, Shi C, Croce K, Zago AC, Lopez J, Andre P, Plow E, Simon DI. Leukocyte engagement of platelet glycoprotein Iba α via the integrin Mac-1 is critical for the biological response to vascular injury. *Circulation.* 2005; 112:2993–3000. [PubMed: 16260637]
38. Ahn GO, Tseng D, Liao CH, Dorie MJ, Czechowicz A, Brown JM. Inhibition of Mac-1 (CD11b/CD18) enhances tumor response to radiation by reducing myeloid cell recruitment. *Proc Natl Acad Sci U S A.* 2010; 107:8363–8. [PubMed: 20404138]
39. Shao B, Wahrenbrock MG, Yao L, David T, Coughlin SR, Xia L, Varki A, McEver RP. Carcinoma mucins trigger reciprocal activation of platelets and neutrophils in a murine model of Trousseau syndrome. *Blood.* 2011; 118:4015–23. [PubMed: 21860019]
40. Phillips JW, Barringhaus KG, Sanders JM, Hesselbacher SE, Czarnik AC, Manka D, Vestweber D, Ley K, Sarembock IJ. Single injection of P-selectin or P-selectin glycoprotein ligand-1 monoclonal antibody blocks neointima formation after arterial injury in apolipoprotein E-deficient mice. *Circulation.* 2003; 107:2244–9. [PubMed: 12707243]
41. Kisucka J, Butterfield CE, Duda DG, Eichenberger SC, Saffaripour S, Ware J, Ruggeri ZM, Jain RK, Folkman J, Wagner DD. Platelets and platelet adhesion support angiogenesis while preventing excessive hemorrhage. *Proc Natl Acad Sci U S A.* 2006; 103:855–60. [PubMed: 16418262]
42. von Drygalski A, Furlan-Freguia C, Ruf W, Griffin JH, Mosnier LO. Organ-Specific Protection Against Lipopolysaccharide-Induced Vascular Leak Is Dependent on the Endothelial Protein C Receptor. *Arterioscler Thromb Vasc Biol.* 2013; 33:769–76. [PubMed: 23393392]
43. Riewald M, Ruf W. Protease-activated receptor-1 signaling by activated protein C in cytokine-perturbed endothelial cells is distinct from thrombin signaling. *J Biol Chem.* 2005; 280:19808–14. [PubMed: 15769747]
44. Riewald M, Petrovan RJ, Donner A, Mueller BM, Ruf W. Activation of endothelial cell protease activated receptor 1 by the protein C pathway. *Science.* 2002; 296:1880–2. [PubMed: 12052963]

45. Qian BZ, Li J, Zhang H, Kitamura T, Zhang J, Campion LR, Kaiser EA, Snyder LA, Pollard JW. CCL2 recruits inflammatory monocytes to facilitate breast-tumour metastasis. *Nature*. 2011; 475:222–5. [PubMed: 21654748]
46. Labelle M, Begum S, Hynes RO. Direct Signaling between Platelets and Cancer Cells Induces an Epithelial-Mesenchymal-Like Transition and Promotes Metastasis. *Cancer Cell*. 2011; 20:576–90. [PubMed: 22094253]

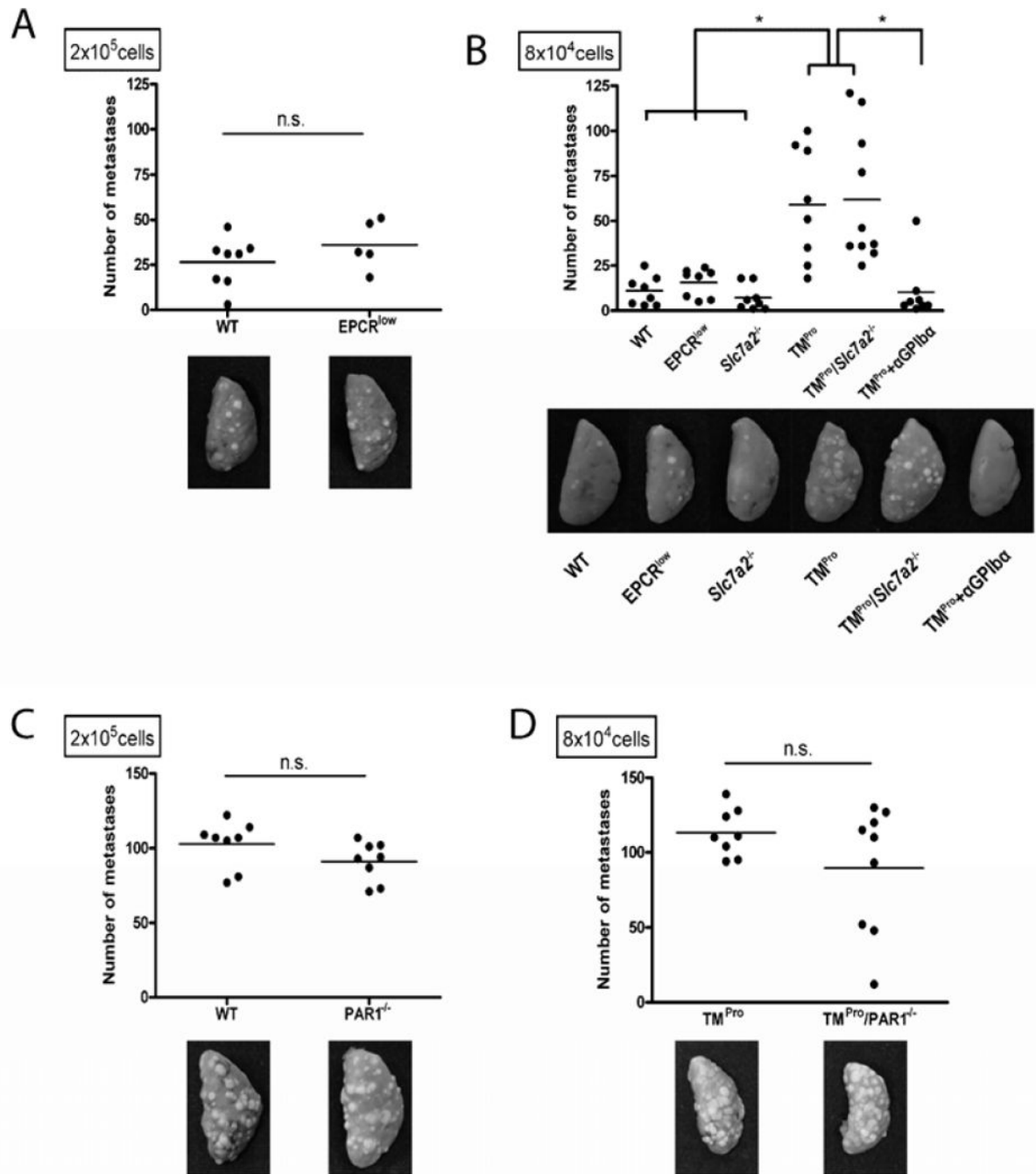


Fig. 1. Extrinsic coagulation activation solely promotes metastasis in WT and TM^{Pro} mice
 (A) Metastasis of PyMT breast cancer cells in WT and TM^{Pro} mice, * $p < 0.0001$, t-test. (B, C, D) Efficient deletion of TF by cre recombinase transfection of PyMT-TF^{fllox} breast cancer cells by Western blotting (B), FACS analysis (C), and FXa generation assay (D), * $p < 0.001$, t-test. (E) Pulmonary metastases counts and representative views of wild type (WT) and TM^{Pro} mice challenged with 2×10^5 PyMT-TF^{fllox} control or cre+ adenovirus-treated cells, * $p < 0.001$, ANOVA. (F) Reconstitution of fITF and asTF in cre recombinase-treated PyMT-TF^{fllox} cells verified by Western blotting of total cell lysates (cells), conditioned medium (CM) and the derived MP fraction (MP) and MP-depleted supernatant (Sup). (G) Pulmonary

metastasis of cells reconstituted with full-length murine TF (mTF) or alternatively spliced TF (asTF). Control cells were transduced with empty retrovirus (mock), $*p < 0.001$, ANOVA. (H) Metastasis in mice with or without inhibition of contact pathway-dependent FXI activation with anti-XI antibody 14E11; comparison of treated and untreated mice by t-test, $p > 0.05$.

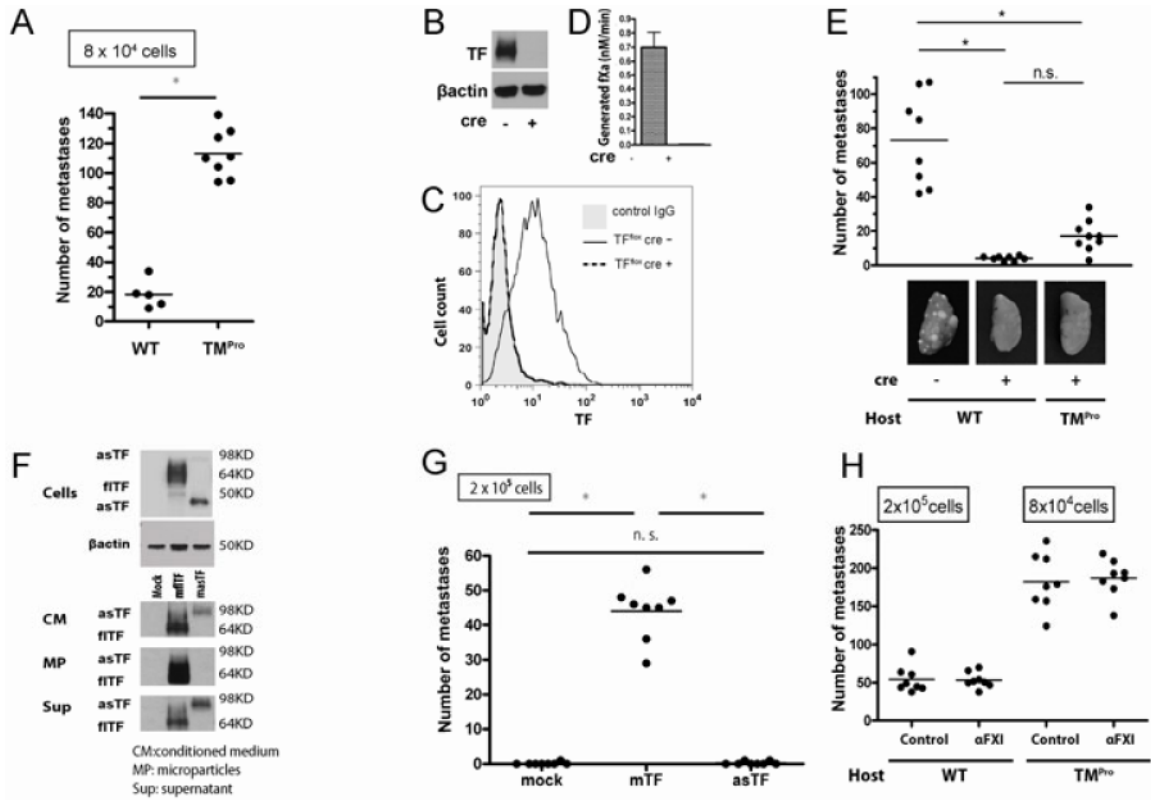


Fig. 2. TM^{Pro} mice have hyper-reactive platelets

(A) Metastases in fibrinogen-depleted WT or TM^{Pro} mice challenged with 2×10^5 or 8×10^4 PyMT- TF^{flx} cells, respectively; * $p = 0.00034$ for WT and $p = 0.069$ for TM^{Pro} , t-test. (B) Effect of fibrin depletion on platelet counts, mean \pm SEM, $n = 3$; control versus depleted TM^{Pro} at 4 hours $p < 0.001$, ANOVA. (C–E) Effect of tumor cell injection (2×10^5 /mouse) on platelet PS exposure, $p = 0.0024$, ANOVA (C), counts, (D) and circulating platelet-leukocyte aggregates $p < 0.0001$, ANOVA (E) evaluated after 2 hours with the depicted number of animals. Control experiments in $TM^{Pro}/PAR1^{-/-}$ mice showed that platelet responses were independent of PAR1 signaling, as expected.

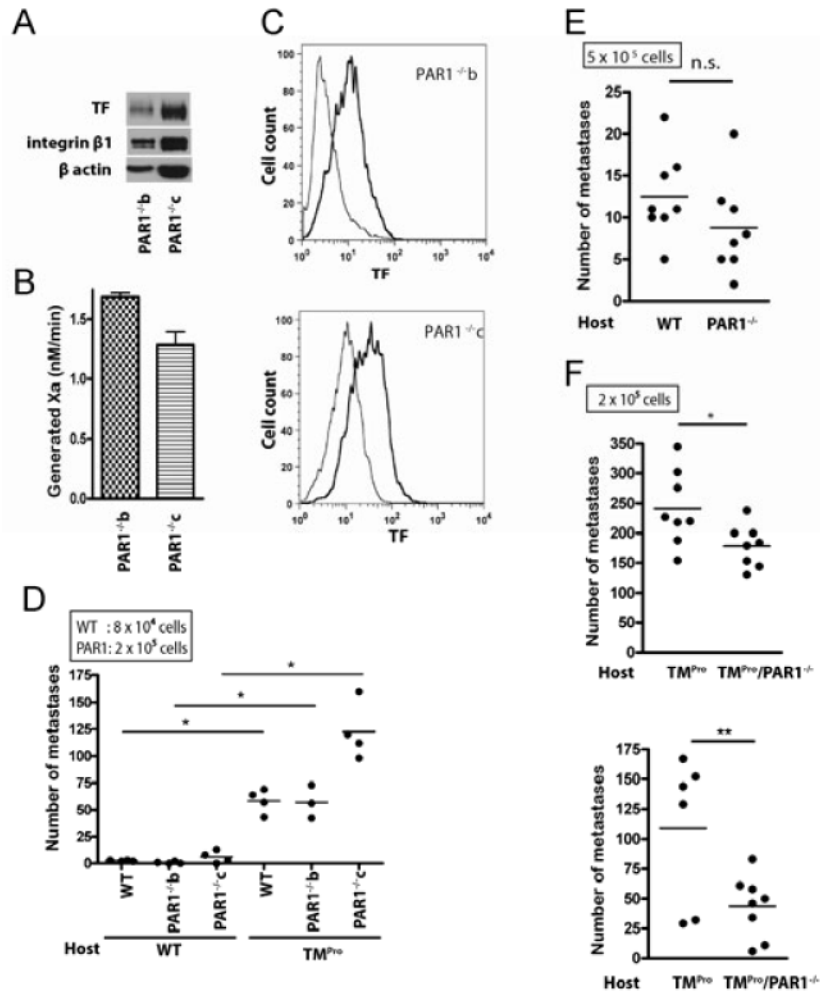


Fig. 3. Enhanced metastasis in TM^{Pro} mice is independent of platelet GPIIb/IIIa interaction with CD11b

(A) Metastasis of 2×10^5 or 8×10^4 PyMT-TF^{fllox} cells injected into WT or TM^{Pro} mice, respectively, following treatment with anti-CD11b antibody M1/70 or isotype control rat IgG2b; or (B) of 8×10^4 PyMT-TF^{fllox} cells injected into TM^{Pro} mice following blockade of PSGL-1 or PSGL-1 and CD11b. (C) Platelet counts following depletion with anti-mouse GPIIb/IIIa antibody 5A7 and transfusion of platelets with human GPIIb/IIIa (6.2×10^8 platelets/mouse) or an IL-4R chimeric receptor (4.8×10^8 platelets/mouse), mean \pm SEM, n = 4. (D) Tumor cell retention quantified by real-time PCR 24 hours after injection of 5×10^5 PyMT-TF^{fllox} cells into untreated or platelet-depleted WT mice; * $p < 0.001$, t-test. (E) Metastasis following injection of 2×10^5 PyMT-TF^{fllox} cells after platelet reconstitution of WT mice with 6×10^8 platelets/mouse; no Plts versus control $p < 0.01$, versus hGPIIb/IIIa Plts $p < 0.001$, versus IL-4R Plts $p < 0.05$. Metastasis following injection of 8×10^4 PyMT-TF^{fllox} cells into TM^{Pro} mice reconstituted with 4×10^8 platelets/mouse; no Plts versus control or hGPIIb/IIIa Plts $p < 0.001$, versus IL-4R Plts $p < 0.01$; ANOVA with Bonferroni post test.

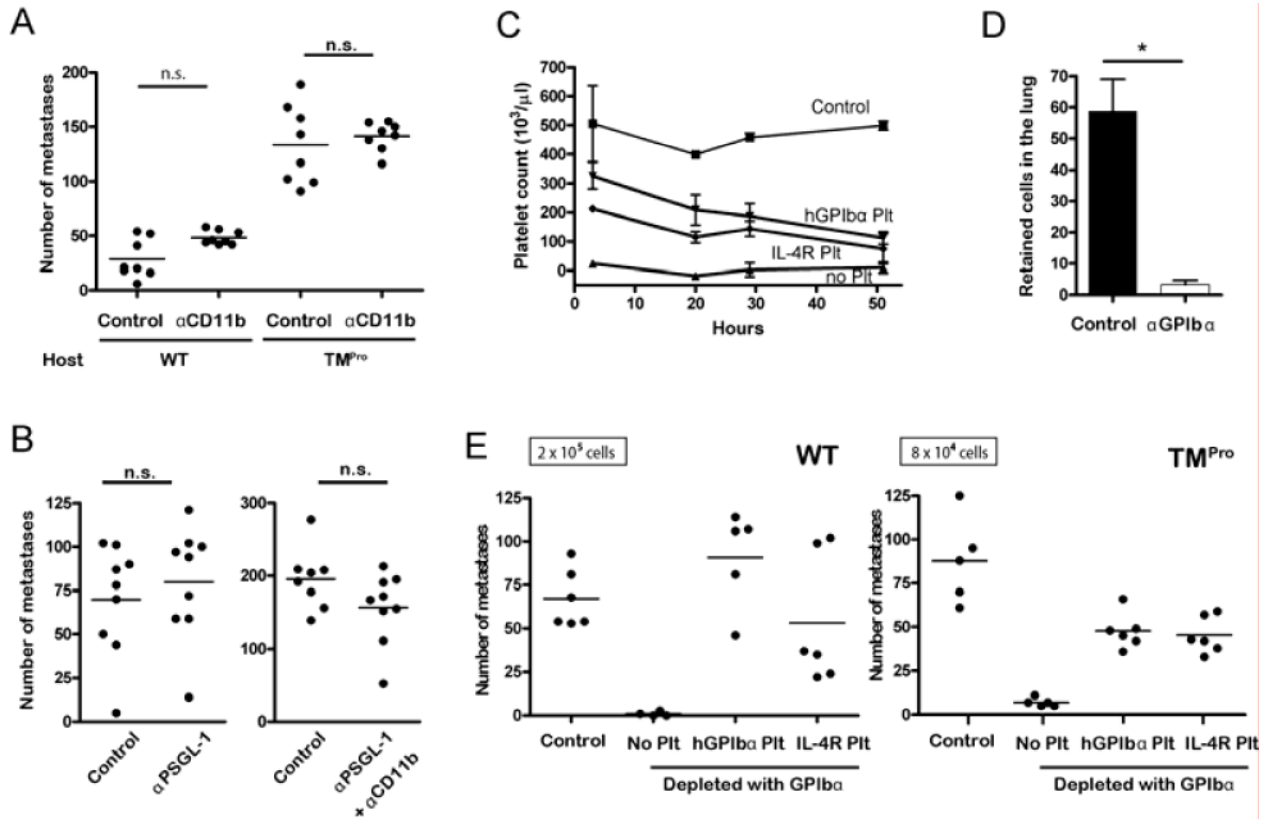


Fig. 4. Endothelial cell thrombin signaling targets are not required for metastasis in TM^{Pro} mice
 (A) Metastasis following injection of PyMT- TF^{lox} cells is not increased in $EPCR^{low}$ mice.
 (B) Deletion of the thrombin target gene *Slc7a2* does not reduce metastasis in TM^{Pro} mice. Metastases numbers and appearance in WT, $EPCR^{low}$, $Slc7a2^{-/-}$, TM^{Pro} , $TM^{Pro}/Slc7a2^{-/-}$, and platelet-depleted TM^{Pro} mice; * $p < 0.001$; ANOVA. Results for TM^{Pro} and $TM^{Pro}/Slc7a2^{-/-}$ mice were confirmed in an independent experiment. (C) Metastasis in WT and $PAR1^{-/-}$ mice. (D) Metastasis of PyMT- TF^{lox} cells in TM^{Pro} and $TM^{Pro}/PAR1^{-/-}$ mice. These results were independently reproduced.

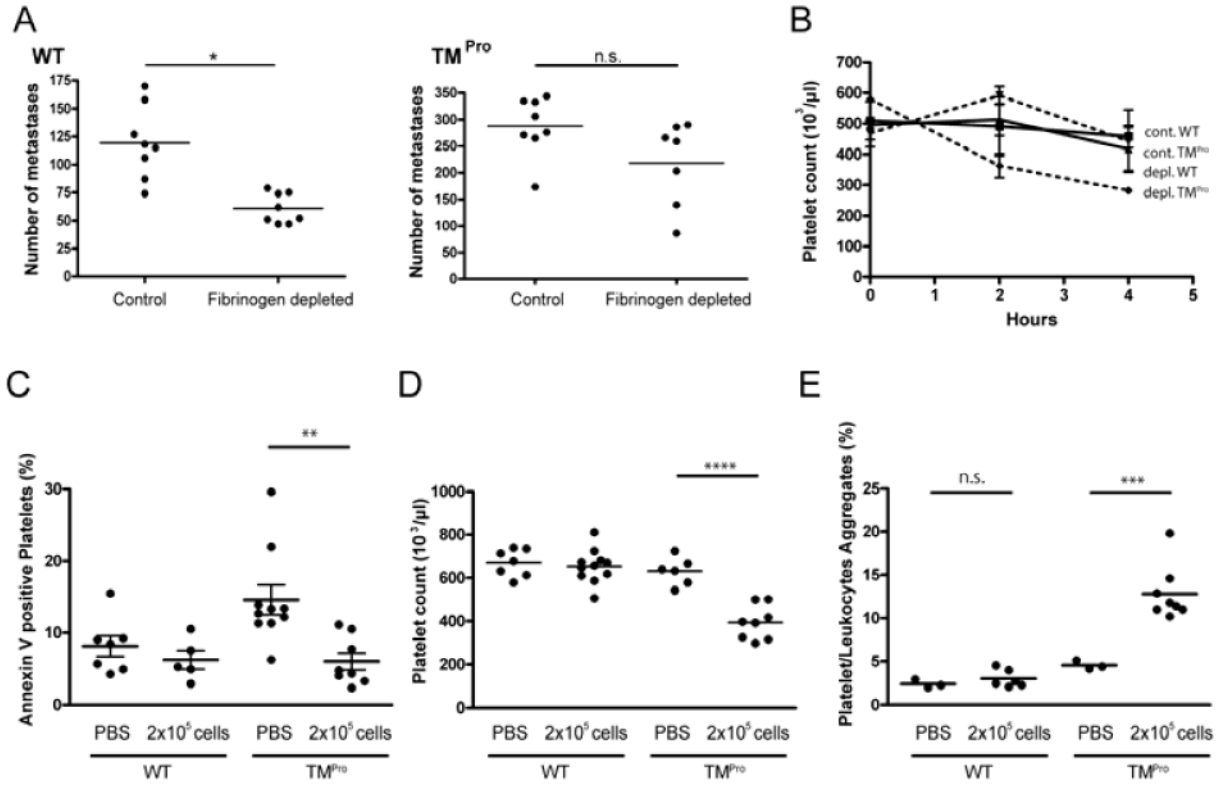


Fig. 5. Redundant roles of tumor and host PAR1 signaling in enhanced metastasis in TM^{Pro} mice

(A) TF and integrin $\beta 1$ levels of PyMT-PAR1^{-/-} lines derived from two independent tumor-bearing mice (PAR1^{-/-b}, PAR1^{-/-c}) determined by Western blotting. (B) TF activity of PAR1^{-/-} lines determined by FXa generation assay. (C) FACS analysis of TF expression by PAR1^{-/-b}, and PAR1^{-/-c} cells. (D) Metastasis in WT or TM^{Pro} mice following injection of 2×10^5 PAR1^{-/-b} and PAR1^{-/-c} cells or 8×10^4 PyMT-TF^{flox} cells (WT), * $p < 0.001$ t-test. (E) Effect of host PAR1-deficiency on metastasis of 5×10^5 PAR1^{-/-c} cells injected into WT or PAR1^{-/-} mice. (F) Effect of host PAR1-deficiency on metastasis of 2×10^5 PAR1^{-/-c} cells injected into TM^{Pro} or TM^{Pro}/PAR1^{-/-} mice; * $p = 0.027$, ** $p = 0.019$, t-test. In a third experiment with smaller groups, a similar trend was observed.